High level production of amorphadiene using Bacillus subtilis as an optimized terpenoid cell factory

Pramastya, Hegar; Xue, Dan; Abdallah, Ingy I; Setroikromo, Rita; Quax, Wim J

Published in:
New Biotechnology

DOI:
10.1016/j.nbt.2020.10.007

Publication date:
2021

New BIOTECHNOLOGY 60 (2021) 159–167

Contents lists available at ScienceDirect

New BIOTECHNOLOGY

journal homepage: www.elsevier.com/locate/nbt

Full length Article

High level production of amorphadiene using *Bacillus subtilis* as an optimized terpenoid cell factory

Hegar Pramastya [a,b,1], Dan Xue [a,1], Ingy I. Abdallah [a,c], Rita Setroikromo [a], Wim J. Quax [a,*]

[a] Department of Chemical and Pharmaceutical Biology, Groningen Research Institute of Pharmacy, University of Groningen, 9713 AV, Groningen, the Netherlands
[b] Pharmaceutical Biology Research Group, School of Pharmacy, Institut Teknologi Bandung, 40132, Bandung, Indonesia
[c] Department of Pharmacognosy, Faculty of Pharmacy, Alexandria University, Egypt

ARTICLE INFO

Keywords:
Artemisinin
Amorphadiene
Bacillus subtilis
MEP pathway
Response surface method

ABSTRACT

The anti-malarial drug artemisinin, produced naturally in the plant *Artemisia annua,* experiences unstable and insufficient supply as its production relies heavily on the plant source. To meet the massive demand for this compound, metabolic engineering of microbes has been studied extensively. In this study, we focus on improving the production of amorphadiene, a crucial artemisinin precursor, in *Bacillus subtilis*. The expression level of the plant-derived amorphadiene synthase (ADS) was upregulated by fusion with green fluorescent protein (GFP). Furthermore, a co-expression system of ADS and a synthetic operon carrying the 2-C-methyl-D-erythritol-4-phosphate (MEP) pathway genes was established. Subsequently, farnesyl pyrophosphate synthase (FPPS), a key enzyme in formation of the sesquiterpene precursor farnesyl pyrophosphate (FPP), was expressed to supply sufficient substrate for ADS. The consecutive combination of these features yielded a *B. subtilis* strain expressing chromosomally integrated GFP-ADS followed by FPPS and a plasmid encoded synthetic operon showing a stepwise increased production of amorphadiene. An experimental design-aided systematic medium optimization was used to maximize the production level for the most promising engineered *B. subtilis* strain, resulting in an amorphadiene yield of 416 ± 15 mg/L, which is 20-fold higher than that previously reported in *B. subtilis* and more than double the production in *Escherichia coli* or *Saccharomyces cerevisiae* on a shake flask fermentation level.

Introduction

Terpenoids are considered, functionally and structurally, the largest and most diverse group among natural products. In spite of their diversity, the backbone of all terpenoids is constructed by consecutive condensation of two C_5 precursors, isopentenyl pyrophosphate (IPP) and its isomer dimethylallyl pyrophosphate (DMAPP). In eukaryotes and certain prokaryotes including archaebacteria, these C_5 precursors are mainly produced via the mevalonate (MVA) pathway, while in prokaryotes and plastids of plant cells, it is via the 2-C-Methyl-D-erythritol-4-phosphate (MEP) pathway. The number of known terpenoids currently characterized is over 50,000 compounds widespread among living organisms. Several terpenoids are commercially well known for their nutritional or medicinal applications. Among medically important terpenoids, the antimalarial artemisinin and the anticancer drug Taxol® are prime examples. Most terpenoids are produced naturally in low quantities and extraction from their biological material usually gives a low and fluctuating yield in spite of a substantial consumption of natural resources. Moreover, the complex structures of terpenoids cause their chemical synthesis to be problematic and expensive. Thus, there is a pressing need for alternative methods for production of terpenoids and as a result there has been a focus on the metabolic engineering of microbial hosts to act as cell factories for terpenoid production [1–11].

Since 2002, the WHO has recommended artemisinin-based combination therapy (ACT) as the first line for the treatment of uncomplicated *Plasmodium falciparum* malarial infection [12]. The demand for ACTs

Abbreviations: MEP, 2-C-methyl-D-erythritol-4-phosphate; IPP, isopentenyl pyrophosphate; DMAPP, dimethylallyl pyrophosphate; GRAS, generally regarded as safe; ADS, amorphadiene synthase; GFP, green fluorescent protein; FPPS, farnesyl pyrophosphate synthase; GC–MS, Gas chromatography–mass spectrometry; CCD, central composite designs; RSM, response surface method; OPT, optimized culture medium.

* Corresponding author at: Antonius Deusinglaan 1, Building 3215, room 917, 9713AV, Groningen, the Netherlands.
E-mail address: w.j.quax@rug.nl (W.J. Quax).

[1] Hegar Pramastya and Dan Xue contributed equally to this work.

https://doi.org/10.1016/j.nbt.2020.10.007
Received 15 January 2020; Received in revised form 15 October 2020; Accepted 16 October 2020
Available online 22 October 2020

since then has kept increasing and it is predicted to reach 800 million ACT packages by 2021 [13]. Similar to the majority of terpenoids, relying on the plant source for commercial production of artemisinin has usually led to fluctuations in price and shortfalls in production of such an important medicine. Hence, semi-synthetic artemisinin production using microbial cell factory could be an alternative choice. Metabolically engineered yeast has been able to produce artemisinic acid, as the closest precursor to artemisinin, up to 25 g/L in a mixed feed two phase fermentation [14].

With its 'generally regarded as safe' (GRAS) status and fast growth rate, *Bacillus subtilis* might be a better choice to produce semi-synthetic artemisinin. Recently, *B. subtilis* garnered interest as a platform organism for terpenoid production. It possesses an endogenous MEP pathway that is capable of producing high amounts of isoprene; in addition, its GRAS status makes it a better choice than *Escherichia coli* and it has been used in industry for decades for large scale fermentations. *B. subtilis* also has a faster growth rate than the yeast *Saccharomyces* cerevisiae that is similarly used as a microbial cell factory. It has been reported that C_{30} carotenoids could be successfully produced in *B. subtilis* by expression of *Staphylococcus crtM* and *crtN* genes and the production of these carotenoids was further enhanced by overexpression of different MEP pathway enzymes [15,16]. Moreover, co-expression of a synthetic operon of the MEP pathway with taxadiene synthase was able to increase the production level of taxadiene as paclitaxel (Taxol®) precursor to up to 17.8 mg/L [17]. Currently, many tools have been established to take *B. subtilis* capability to the next level. Genomic engineering techniques such as CRISPR Cas9 for example have been developed [18,19] and high dynamic promoters which facilitate better tuning of protein expression have been developed, together with a set of regulatory tools such as various ribosome binding sites [20,21]. The advances in the development of genetic methods for manipulation of *B. subtilis* makes it a strong candidate for use as a microbial cell factory that can compete and even exceed the widely researched *E. coli* and *S. cerevisiae* cell factories [22–25].

Amorphadiene is the first committed intermediate in synthesis of artemisinin. It is produced through the amorphadiene synthase (ADS)-catalyzed cyclization of farnesyl pyrophosphate (FPP), which is considered a rate limiting step in artemisinin production. Hence, the first step to establish *B. subtilis* as a cell factory for artemisinin production is the high-level expression of plant derived ADS. In several cases, plant enzymes may be poorly expressed in heterologous microbial hosts [5,6,26–29]. Hence, improving expression of ADS could have a pivotal role in high production of amorphadiene. Recently, modification of the N-terminus of proteins by means of a highly expressed protein tag or a fusion protein partner has been suggested to improve solubility, folding and overall expression of heterologous proteins in *B. subtilis* [22,30–32]. Green fluorescent protein (GFP), as a fusion protein partner, has become well known for its high level expression and correct folding in *B. subtilis*, giving high intensity of fluorescence either at the planktonic or biofilm culture of *B. subtilis* [22].

In this paper, we initially focus on improving the functional expression of ADS in *B. subtilis*, as compared to previous reports, by fusion with GFP. In addition to comparing the expression levels of ADS and the GFP-ADS fusion, plasmid-based and chromosomally integrated gene expression were also evaluated. The amount of amorphadiene produced by the different strains was improved by combination with a synthetic operon overexpressing all the MEP pathway enzymes and farnesyl pyrophosphate synthase (FPPS) in order to optimize the flux via the metabolic pathway. Finally, to ensure the highest production, factors affecting amorphadiene yield were systematically screened and optimized.

Methods

Bacterial strains, plasmids, and media

Bacterial strains and plasmids used in this paper are listed in Table 1. *E. coli*DH5α strains were grown in Luria-Bertani broth (LB). *B. subtilis* 168 strains were cultured in 2YT (1.6 % Bacto-tryptone, 1 % Bacto-yeast extract, 0.5 % NaCl, pH 7.0), 2PY (2 % peptone, 1 % Bacto-yeast extract, 1 % NaCl, pH 7.0), TSB (17 g/L tryptone, 3 g/L soytone, 2.5 g/L dextrose, 5.0 g/L NaCl, 2.5 g/L K_2HPO_4) or 2SR (3 % Bacto-tryptone, 5 % Bacto-yeast extract, 0.6 % K_2HPO_4, pH 7.0) as required. Antibiotics were added to media as necessary: 100 μg/mL ampicillin or 100 μg/mL erythromycin for *E. coli* DH5α and 5 μg/mL chloramphenicol, 10 μg/mL erythromycin or 10 μg/mL spectinomycin for *B. subtilis* 168. Glycerol, Na pyruvate, K_2HPO_4, $MgCl_2$, $MnCl_2$, $CoCl_2$ and NH_4Cl were used for medium optimization. Reagents, antibiotics and culture media components were purchased from Duchefa, Harlem, The Netherlands or Merck, Amsterdam, The Netherlands.

Cloning and engineering of B. subtilis strains

ads and *gfp-ads* genes were cloned into pDR111 and pBS0E plasmids by restriction dependent or circular polymerase extension cloning (CPEC) [33]. The *gfp* gene was codon optimized for *Streptococcus pneumoniae*. The *fpps* gene from *Saccharomyces cerevisiae* was inserted downstream of the *gfp-ads* gene into both plasmids by using the CPEC protocol [33]. Plasmids were transferred into *B. subtilis* by chemically induced transformation following Anagnostopoulos protocol (full details are available in the supplementary information) [25]. Prior to transformation, the pDR111 plasmid required linearization at a *Stu*I restriction site. To overexpress the MEP pathway, three constructs of pHCMC04G plasmids containing partial and whole MEP pathway genes (Fig. 1) in operons controlled by a xylose inducible promoter, namely the SDFH operon harboring *dxs*, *ispD*, *ispF* and *ispH*, the CEGA operon harboring *ispC*, *ispE*, *ispG* and *ispA*, and the SDFHCEGA operon carrying all eight genes, were co-transformed to the *B. subtilis* strains harboring *ads* or *gfp-ads* gene. At the end, twelve strains of *B. subtilis* 168 were produced by transforming different combinations of the constructs (Table 2).

Growth conditions and amorphadiene extraction

Overnight cultures of the *B. subtilis* strains were diluted 50x in the selected medium to a final volume of 1 mL (in 14 mL round-bottom tubes) or 10 mL (in 100 mL Erlenmeyer flasks) and OD_{600} of around

Table 1
Bacterial strains and vectors used in this research.

Bacterial strain	Genotype	References
B. subtilis 168	*trp*C2	[39,40]
Bsu_ads	168 *amyE*::$P_{hyperspank}$ *ads*; Sp^R	This study
*Bsu*_gfp-ads	168 *amyE*::$P_{hyperspank}$ *gfp-ads*; Sp^R	This study
*Bsu*_gfp-ads + fpps	168 *amyE*::$P_{hyperspank}$ *gfp-ads* + *fpps*; Sp^R	This study
E. coli DH5α	F^-*end*A1 *hsd*R17 (r_k^-,m_k^+) *sup*E44 *thi*$^-$1 λ$^-$*rec*A1 *gyr*A96 *rel*A1 φ80d*lac*ZΔM15	Bethesda Research Lab 1986
Plasmid	**Pertinent properties**	**Reference**
pDR111	*B. subtilis* integration vector; ori-pBR322; $P_{hyperspank}$ IPTG-inducible promoter; Sp^R; Amp^R	[22]
pBS0E	*B. subtilis* and *E. coli* shuttle vector; ori-ColE1; ori- 1030 (theta replication); P_{xylA} xylose-inducible promoter; Erm^R; Amp^R	[23]
pHCMC04G	*B. subtilis* and *E. coli* shuttle vector; ori-pBR322; ori-pBS72 (theta replication); P_{xylA} xylose-inducible promoter; Cm^R; Amp^R	[16]

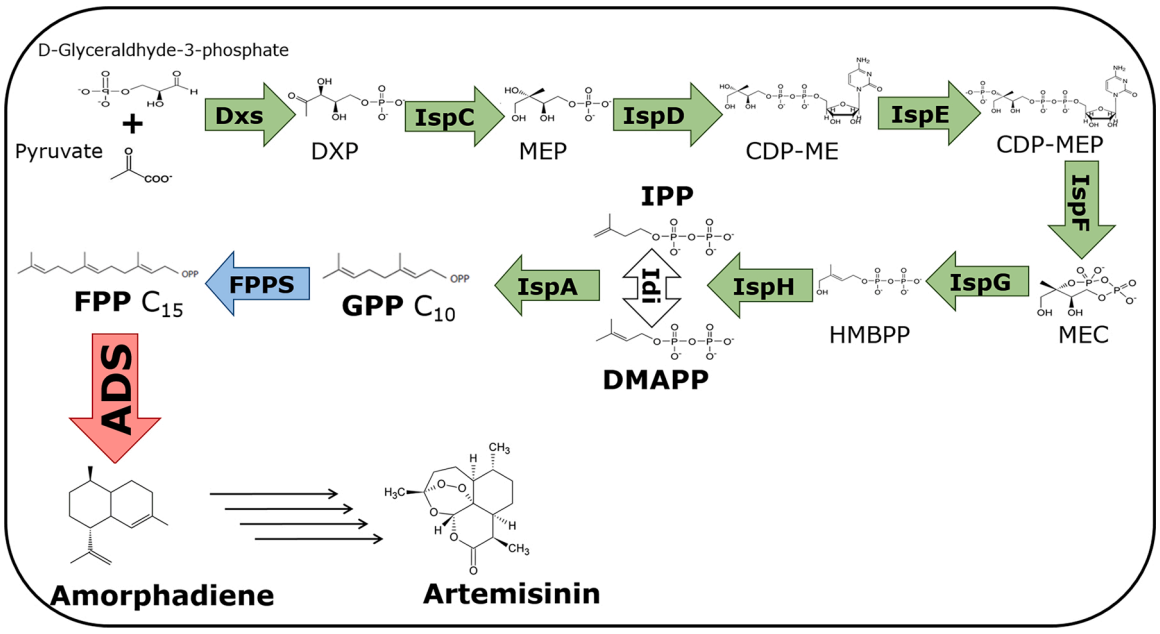

Fig. 1. Biosynthesis of amorphadiene (first committed precursor in artemisinin biosynthesis) via the 2-C-methyl-D-erythritol-4-phosphate (MEP) pathway in *Bacillus subtilis* cGAF/SDFHCEGA strain. **Intermediates:** 1-deoxy-D-xylulose 5-phosphate (DXP), 2-C-methyl-D-erythritol 4-phosphate (MEP), 4-(cytidine 5′-diphospho)-2-C-methyl-D-erythritol (CDP-ME),2-phospho-4-(cytidine 5′-diphospho)-2-C-methyl-D-erythritol (CDP-MEP), 2-C-methyl-D-erythritol 2,4-cyclodiphosphate (MEC), (E)-4-hydroxy-3-methylbut-2-en-1-yl diphosphate (HMBPP), isopentenyl diphosphate (IPP), dimethylallyl diphosphate (DMAPP), geranyl pyrophosphate (GPP) and farnesyl pyrophosphate (FPP). **Enzymes (genes):** 1-deoxy-D-xylulose-5-phosphate synthase (Dxs), 1-deoxy-D-xylulose-5- phosphate reductoisomerase, or 2-C-methyl-D-erythritol 4-phosphate synthase (Dxr, IspC), 2-C-methyl-D-erythritol 4-phosphate cytidylyltransferase (IspD), 4-(cytidine 5′-diphospho)-2-C-methyl-D-erythritol kinase (IspE), 2-C-methyl-D-erythritol 2,4-cyclodiphosphate synthase (IspF), (E)-4-hydroxy-3-methylbut-2-enyldiphosphate synthase (IspG), 4-hydroxy-3-methylbut-2-enyl diphosphate reductase (IspH), isopentenyldiphosphate delta-isomerase (Idi), IspA which act as geranyl pyrophosphate synthase and farnesyl pyrophosphate synthase, Saccharomyces cerevisiae farnesyl pyrophosphate synthase (FPPS) and amorphadiene synthase (ADS).

Table 2
Strains constructed in this study.

Strains*	Vector	Genes
pA	pBS0E	*ads*
pGA	pBS0E	*gfp-ads*
pGA/CEGA	pBS0E	*gfp-ads*
	pHCMC04G	*ispC+ispE+ispG+ispA*
pGA/SDFH	pBS0E	*gfp-ads*
	pHCMC04G	*dxs+ispD+ispF+ispH*
pGA/SDFHCEGA	pBS0E	*gfp-ads*
	pHCMC04G	*dxs+ispD+ispF+ispH+ispC+ispE+ispG+ispA*
pGAF/SDFHCEGA	pBS0E	*gfp-ads + fpps*
	pHCMC04G	*dxs+ispD+ispF+ispH+ispC+ispE+ispG+ispA*
cA	pDR111	*ads* in chromosome
cGA	pDR111	*gfp-ads* in chromosome
cGA/CEGA	pDR111	*gfp-ads* in chromosome
	pHCMC04G	*ispC+ispE+ispG+ispA*
cGA/SDFH	pDR111	*gfp-ads* in chromosome
	pHCMC04G	*dxs+ispD+ispF+ispH*
cGA/ SDFHCEGA	pDR111	gfp-ads in chromosome
	pHCMC04G	*dxs+ispD+ispF+ispH+ispC+ispE+ispG+ispA*
cGAF/ SDFHCEGA	pDR111	*gfp-ads + fpps* in chromosome
	pHCMC04G	*dxs+ispD+ispF+ispH+ispC+ispE+ispG+ispA*

* Strain names starting with "p" indicated *ads*, *gfp-ads* genes or *gfp-ads + fpps* operon located in the replicating plasmid pBS0E, those names beginning with "c" depicted genes or operon that were integrated into the chromosome of *B. subtilis*.

0.1. The expression cultures were incubated at 37 °C, and 220 rpm until OD_{600} 0.7−1. Then cultures were induced by 1 % xylose for strains bearing pHCMC04G and pBS0E plasmids and 1 mM IPTG for pDR111 strains, and 15 % (v/v) dodecane (Sigma-Aldrich, Zwijndrecht, The Netherlands) containing 56 mg/L *β*-caryophyllene as internal standard was added to the cultures to trap the amorphadiene produced. After induction, the cultures were grown for 24 or 48 h at 20 °C and 220 rpm. The cultures and dodecane layers were collected as needed.

Extracellular amorphadiene was trapped by dodecane during culture growth. To extract intracellular amorphadiene, the culture was first centrifuged at 16,200 xg for 15 min, then the supernatant was removed and the pellet was resuspended in lysis buffer [50 mM glucose, 25 mM Tris pH 8.0, 1 cOmplete™ Protease Inhibitor Cocktail tablet (1 tablet per 50 mL), 0.25 mg/mL lysozyme, 20 mM $MgCl_2$, 0.01 % DNAse 2000 units/mg (Sigma-Aldrich, Zwijndrecht, The Netherlands)] with 200 µL dodecane containing internal standard. The resuspended pellets were incubated at 37 °C for 30 min with 220 rpm shaking. The mixtures of the cell lysate and dodecane were centrifuged for 10 min at 11,600 xg, then the dodecane layer was decanted for further GC–MS analysis (below).

Real-time quantitative PCR (qPCR) analysis

Total RNA was isolated from each of the strains after 5 h incubation following induction using Maxwell 16 LEV simply RNA purification kit (Promega, Leiden, The Netherlands). The isolated total RNA was directly processed through reverse transcription facilitated by random primers to produce cDNA. Real-time qPCR with SensiMix™ SYBR LowROX kit (Bioline, UK) was conducted to measure the transcript level. The absolute quantitation method was applied to analyze the transcription level of *ads* and MEP pathway genes, which was expressed as the log10 of the absolute copy number per unit input total cDNA (10 ng) (full details are available in the supplementary information).

Western blot analysis

Cells were pelleted from the cultures after 24 h growth in which the volume was normalized to OD_{600} = 1. The pellets were lysed by lysis buffer containing: 50 mM glucose, 25 mM Tris pH 8.0, 1 cOmplete™ Protease Inhibitor Cocktail tablet from Sigma-Aldrich (1 tablet per 50 mL), 0.25 mg/mL lysozyme, 20 mM $MgCl_2$, DNAse 0.01 %; and

incubated for 30 min at 37 °C. The protein concentration was measured by Bradford assay (Thermo-Fisher Scientific, Groningen, The Netherlands) and 40 μg of protein lysate samples were loaded onto an SDS PAGE gel, 4–12 % NuPAGE Bis-Tris precast gel system in NuPAGE MOPS running buffer solution (Thermo-Fisher Scientific, Groningen, The Netherlands), and run at 100 V for approximately 1 h. The protein was transferred to methanol activated PVDF membrane (Sigma-Aldrich, Zwijndrecht, The Netherlands) in cold transfer buffer [3.1 g tris-base, 11.3 g glycine dissolved in 800 mL deionized water with 200 mL methanol (Duchefa, Harlem, The Netherlands), pH 7.6] for 1 h at 100 V. Then, the membrane was incubated with Blocking Buffer solution for fluorescent western blot (Rockland, MB-070) before incubation with primary and secondary antibodies. For detection of ADS, a special request proprietary rabbit polyclonal anti-ADS antibody, ordered and prepared using purified ADS protein (Davids Biotechnology GmbH, Regensburg, Germany), was used as primary antibody at a dilution of 1:80. The secondary antibody was IRDye800 CW goat anti-rabbit IgG (Li-COR Biosciences, Bad Homburg, Germany, cat. No: 926-32211), 1:10,000 dilution.

Gas chromatography – mass spectrometry (GC–MS) analysis of amorphadiene

Amorphadiene measurement was conducted according to published method [34]. The dodecane layer was diluted to an amorphadiene concentration in the range 3.5−28 mg/L. Analysis was performed using a Shimadzu GCMS-QP5000 system equipped with a 17A gas chromatograph (GC) and AOC-20i autoinjector. 2 μL extracts were injected splitless onto an Rx5-ms column (crossbond diphenyl dimethyl polysiloxane). Injector temperature was 250 °C, column temperature was started at 100 °C for 3 min, then gradually increased to 130 °C at a rate of 15 °C/min, and followed by a rate of 5 °C/min until 180 °C. Thereafter, the temperature was increased to 280 °C at a rate of 20 °C/min, and held for 10 min. The MS detector was set to selected ion mode (SIM) monitoring *m/z* ion 189. The concentration of amorphadiene was calculated from *β*-caryophyllene (Extrasynthese, Lyon, France) standard curve and expressed as *β*-caryophyllene equivalent [17].

Analysis of segregational stability of the constructs in cGAF/SDFHCEGA B. subtilis strain

Analysis of segregational stability was conducted for the most promising, cGAF/SDFHCEGA strain. The stability test was conducted in 2YT medium in the absence of antibiotic for 40 generations. Segregational stability depends on the percentage of colonies surviving on antibiotic agar plates. The segregational stability of each construct was represented as the average of the % of colonies retaining the plasmid construct, which is equal to [colonies on 2YT plate with antibiotic / colonies on 2YT plate without antibiotic * 100 %] (full details are available in the supplementary information) [17,35,36].

Medium optimization experimental design and statistical analysis

A medium optimization experiment consisted of primary screening of medium elements, path of steepest ascent, and central composite designs (CCD) and response surface method (RSM). Several elements including carbon source (glycerol), substrate of MEP pathway (pyruvate), buffer (K_2HPO_4), monovalent ion (NH_4^+), and divalent ions (Mn^{2+}, Mg^{2+}, and Co^{2+}) were screened. 2SR medium without K_2HPO_4 was used as the basic medium with pH adjusted to 7.0. Following the preliminary screening by fractional factorial design, the direction of the level of the variables was determined by a path of steepest ascent experiment. Finally, response surface method based on CCD was performed to model and visualize the optimum condition (full details are available in the supplementary information).

Nucleotide sequence accession number

The nucleotide sequence of the amorphadiene synthase gene from *Artemisia annua* was previously reported with accession number **AY006482** [37]. The nucleotide sequence of *gfp* gene was optimized according to codon usage of *Strep.* pneumoniae, as previously reported with accession number **KF410616** [22]. The *fpps* gene was amplified from genomic DNA of *Saccharomyces cerevisiae* with the gene ID **853272** [38]. The nucleotide sequence of the complete genome of *B. subtilis* 168 was previously reported with the accession numbers **AL009126** and **NC_000964** [39–42]. The MEP pathway genes used in this study were amplified from the genomic DNA of *B. subtilis* 168 [16].

Results

Transcription of ads and MEP pathway genes confirmed by qPCR analysis

qPCR was applied to determine the level of transcription of *ads* and MEP pathway genes. The results showed that the *ads* gene is transcribed at a high, almost equal level in each vector system (Fig. 2a). Transcription of *ads* was not significantly altered by constructing the *gfp-ads* fusion. For the assessment of the transcription level of MEP pathway genes, the copy number of the *ispH-ispC* fragment (HC), at the middle of the operon, was quantified as representative for all genes in this construct. Based on previous research, the level of gene expression at the beginning, middle and end of the p04SDFHCEGA operon was compared using the copy numbers of the *dxs-ispD* (SD), *ispH-ispC* (HC) and *ispG-ispA* (GA) fragments and was found to be similar [36]. The use of primers specific for each MEP pathway gene separately was avoided as the presence of a copy of each one in the *B. subtilis* genome would not allow differentiation between transcription of the chromosomal and plasmid genes. The analysis validated the transcription of MEP pathway genes in all strains constructed (Fig. 2b).

Improved expression of ADS by creating a GFP-ADS fusion

The step catalyzed by ADS has been identified as limiting in the biosynthetic pathway of artemisinin [43]. Hence, efforts were made to improve expression of ADS in metabolic pathways as a means of boosting the reaction, including codon usage optimization and construction of a fusion protein. Among them, ADS fusion proteins manifested the most promising improvement of ADS expression and amorphadiene production in *B. subtilis* or *S. cerevisiae* [6,44]. In this study, GFP, codon optimized for *Strep. pneumoniae,* was employed as fusion partner at the N-terminus of ADS to increase the efficiency of translation. This choice was suggested by the report that it exhibited better expression in *B. subtilis* compared to GFP codon optimized for *B. subtilis* [22]. The GFP-ADS fusion protein was considerably more abundant than ADS alone as can be seen from the signal in western blot, indicating that ADS expression was indeed strongly enhanced by N-terminal fusion with GFP (Fig. 3). In line with the hypothesis that more ADS would increase amorphadiene production, the yield of amorphadiene (0.78 mg/L/OD) in strains expressing GFP-ADS fusion increased 2-fold over strains containing ADS alone (0.35 mg/L/OD) (Fig. 3).

Overexpression of all MEP pathway genes together with ispA increased amorphadiene production

As the expression of ADS was significantly increased, the possibility of further improvement of amorphadiene production by increasing the flux through the upstream pathway was tested. In *B. subtilis*, terpenoids are derived from the common C_5 building blocks, IPP and DMAPP, synthesized by its native MEP pathway (Fig. 1). Thus, increasing the supply of the C_5 building blocks could elicit an enhancement in terpenoid production. Our previous study demonstrated that pHCMC04G, a

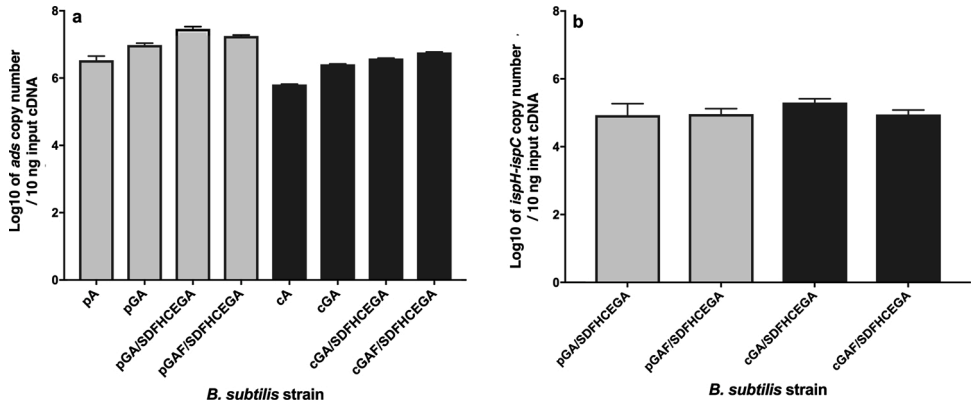

Fig. 2. Expression level of *ads* and MEP pathway genes in *B. subtilis* strains. (**a**) *ads* expression and (**b**) MEP pathway genes expression in *B. subtilis* strains were quantified by RT-qPCR using serial dilutions of standards and depicted as the log10 absolute copy number per unit input total cDNA (10 ng). The data represent the mean with standard deviation, n = 3. For detailed explanation of strain names used, see Table 2.

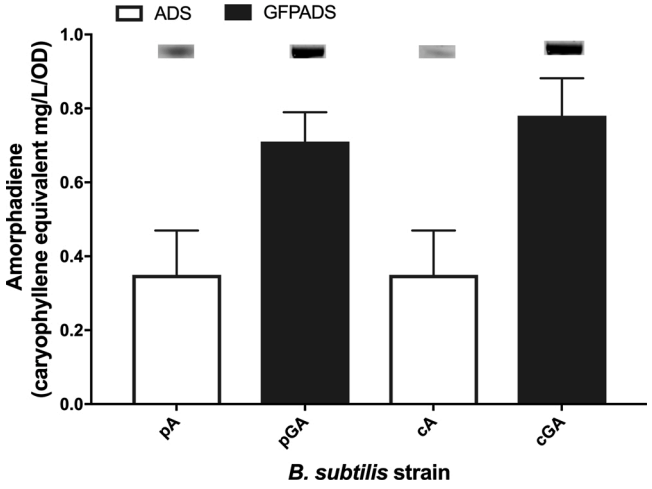

Fig. 3. Comparison of ADS expression and amorphadiene production in ADS and GFP-ADS fusion constructs. Western blot bands above the graph represent ADS or GFP-ADS protein levels of the strains mentioned on the X-axis of the graph. Detection was done with a specially designed proprietary polyclonal antibody against ADS. Each lane contained 40 ng protein from total cell lysate of a 24 h culture. Amorphadiene was collected from 48 h culture in 1 mL 2YT and the concentration of amorphadiene was normalized by OD_{600}. The presented data are average of three replicates, and standard errors were plotted on the graph. Detailed explanation of strain names used can be found in Table 2.

theta replicating plasmid, containing MEP pathway genes significantly boosted production of heterologous terpenoids (C_{30} carotenoids and taxadiene) in *B. subtilis* [16,17]. Here, the plasmid encoding the MEP operon (SDFHCEGA) carrying *dxs*, *ispD*, *ispF*, *ispH*, *ispC*, *ispE*, *ispG* and *ispA,* was combined with the chromosomally encoded ADS constructs. Amorphadiene production was increased by approximately 4-fold in cGA/SDFHCEGA (2.74 mg/L/OD or 35.25 mg/L) compared to cGA (Fig. 4) and by 2-fold over a strain using the construct expressing only four genes of the MEP pathway (cGA/SDFH). A similar pattern can be seen in the strains using a compatible second theta replicating plasmid, pBS0E, to express ADS. The combination of SDFHCEGA and plasmid encoded *ads* gave slightly less product (2.31 mg/L/OD) than that yielded with the chromosomally integrated *ads* (Fig. 4).

Additional expression of FPPS further enhanced yield of amorphadiene

In previous reports in other hosts, heterologous expression of FPPS, a major chain elongation enzyme to form sesquiterpene precursor FPP, was applied to supply sufficient substrate for ADS [45]. Based on preliminary results, FPPS from *S. cerevisiae*, rather than that native to *B. subtilis*, was found to have more impact on amorphadiene synthesis in *B. subtilis* (supplementary Figure S1). Therefore, *S. cerevisiae fpps* was cloned downstream of the *gfp-ads* sequence rendering a single operon, (*gfp-ads* + *fpps*). Upon transfer into *B. subtilis*, noticeable improvement of amorphadiene was indeed found in both cGAF/SDFHCEGA and pGAF/SDFHCEGA strains (Fig. 4) compared to those without the *fpps* constructs ($p < 0.10$). Ultimately, the yield of amorphadiene reached 3.40 mg/L/OD, or 42.50 mg/L.

The constructs in cGAF/SDFHCEGA B. subtilis strain are segregationally stable

Segregational stability is the ability of a bacterial strain to retain at least one plasmid in all daughter cells during cell division, while loss in productivity occurs as plasmid free cells develop. The segregational stability of the cGAF and SDFHCEGA constructs in the cGAF/SDFHCEGA *B. subtilis* strain was evaluated. In the absence of antibiotics, the strain showed a 100 % ability to retain the cGAF construct up to the 40^{th} generation along with a 90 % retention of the SDFHCEGA construct (Fig. 5), which should be adequate for large scale fermentations in the absence of antibiotics [46,47].

Amorphadiene production is strongly boosted through medium optimization

In addition to optimizing the genetic construct, the growth medium was systematically investigated to further boost amorphadiene production. For the most promising strain, cGAF/SDFHCEGA, seven factors, namely glycerol (carbon source), pyruvate (substrate of MEP pathway), K_2HPO_4 (buffer), NH_4^+ (monovalent ion), and Mn^{2+}, Mg^{2+}, Co^{2+} (divalent ions), potentially affecting amorphadiene production were investigated by fractional factorial design (FFD). The optimization was performed based on 2SR medium due to its abundance of carbon and nitrogen source, amino acids and vitamins for bacterial growth. The effects of these variables on the response and significance levels are shown in supplementary Table S4. Statistical analysis identified pyruvate, K_2HPO_4 and Mg^{2+} as the most significant factors for amorphadiene productivity. Pyruvate and K_2HPO_4 exhibited positive effects, whereas Mg^{2+} showed a negative influence. Therefore, they were selected for further optimization.

The path of steepest ascent experiment was applied leading to a maximum production of amorphadiene when the medium was supplemented by 2 % pyruvate, 4 % K_2HPO_4 and no Mg^{2+}, which was chosen as the center point for the next CCD-RSM optimization. The predicted model from the CCD-RSM design was displayed in 3D response surface graphs (Fig. 6). The RSM model predicted a maximum yield of

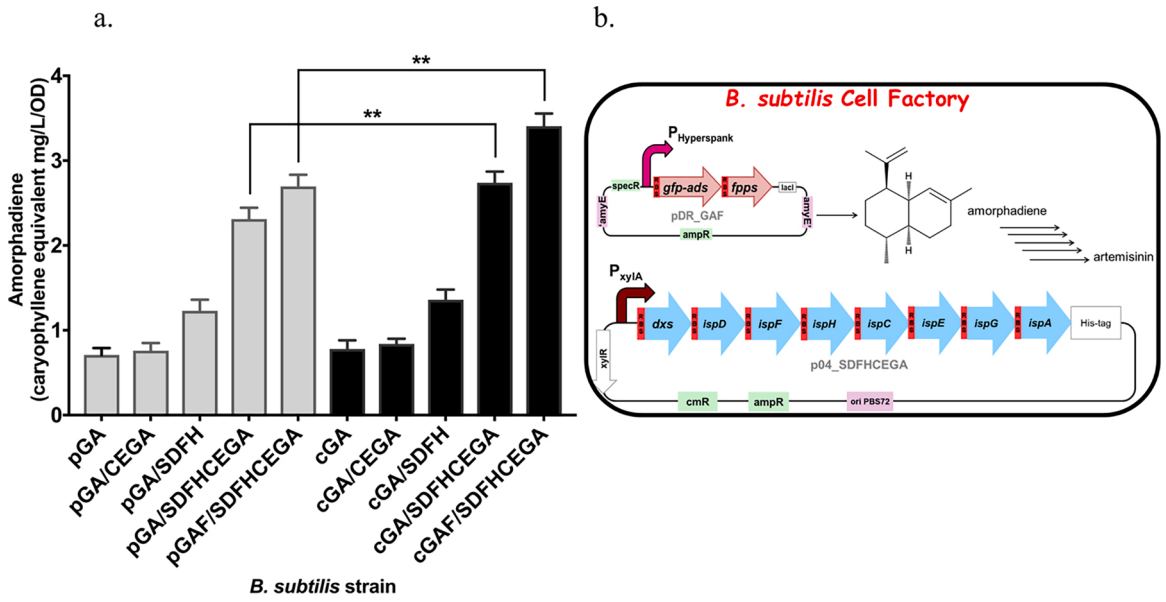

Fig. 4. (**a**) Levels of amorphadiene produced in engineered *B. subtilis* strains with plasmid encoded or chromosomally integrated *ads*. *B. subtilis* strains harboring the *gfp-ads* fusion or *gfp-ads*+*fpps* operon with or without co-expression of MEP pathway genes were cultured in 1 mL 2YT for 48 h, and the concentration of amorphadiene was normalized by OD_{600}. MEP operons were expressed: CEGA contains the genes: *ispC, ispE, ispG* and *ispA*, SDFH contains *dxs*, *ispD*, *ispF* and *ispH* and the SDFHCEGA operon of all 8 genes. The data obtained with plasmid encoded *ads*are in grey, the data with chromosomally integrated *ads* are in black. All data represent the mean with standard deviation, n = 3. ** indicates statistically significant difference ($p < 0.05$). (**b**) Expression vector for *ads* and synthetic operon containing MEP pathway genes in *B. subtilis*. The *gfp-ads* fusion followed by *fpps* gene were integrated into the *B. subtilis* chromosome at the *amyE* locus using pDR111 plasmid. Meanwhile a synthetic operon containing whole MEP pathway genes of *B. subtilis* in addition to *ispA* was carried extra-chromosomally by pHCMC04G plasmid.

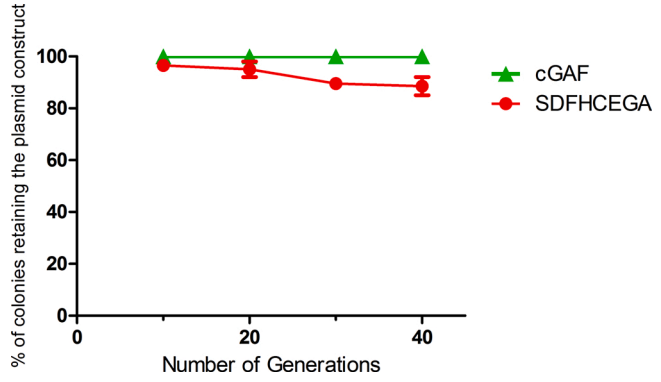

Fig. 5. Segregational stability of cGAF and SDFHCEGA operons in cGAF/SDFHCEGA *B. subtilis* 168 strain. The stability is represented as the % of colonies retaining the plasmid constructs formed on the spectinomycin or chloramphenicol-containing analytical plates, respectively, after successive subculturing in the absence of antibiotics (40 generations). The experiment was performed in duplicate.

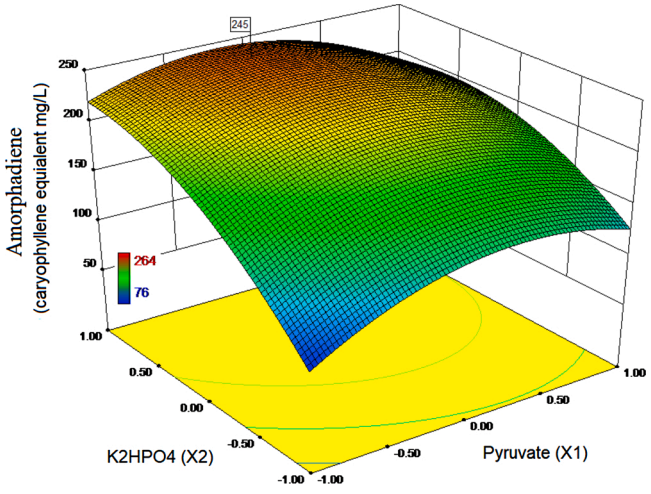

Fig. 6. 3D response surface graphs of pyruvate vs K_2HPO_4 for amorphadiene production. The response surface represents the relationship between the response (AD, amorphadiene, mg/L) and two variables (pyruvate and K_2HPO_4, in code). The highest predicted yield of amorphadiene (mg/L) is marked on the top of the graph.

amorphadiene of 245 mg/L when 1.85 % pyruvate and 4.85 % K_2HPO4 are used. To validate the prediction, cGAF/SDFHCEGA was cultured in optimized medium (designated OPT). The experimental yield of amorphadiene was 258 ± 6 mg/L, thereby validating the model.

The amorphadiene productivity and growth rate of cGAF/SDFHCEGA grown in OPT were compared with other commonly used media (2YT, 2PY, TSB, 2SR) and it was found that OPT was the optimal for amorphadiene production. The yield in OPT was 3-fold and >6-fold higher than that in 2SR and the other tested media, respectively (Fig. 7a). Amorphadiene yields and biomass of cGAF/SDFHCEGA during culturing in 2YT and OPT were measured. Although the amorphadiene accumulation and bacterial growth rate were similar at the beginning of the culture, the yield of amorphadiene and cell density reached a plateau after around 24 h upon using 2YT medium. In OPT both showed a continuous increase and achieved the highest level at around 48 h (Fig. 7b).

Subsequently, the culture volume was scaled up to 10 mL in 100 mL Erlenmeyer shake flasks with OPT and 2YT as control. Similar yields of extracellular amorphadiene were found in either 1 mL or 10 mL cultures. Surprisingly, a remarkable amount of intracellular amorphadiene was detected in OPT at 10 mL but not at 1 mL scale (150 mg/L). In total, the yield of amorphadiene in OPT was 416 ± 15 mg/L (Fig. 8), which is its highest production in *B. subtilis* reported hitherto.

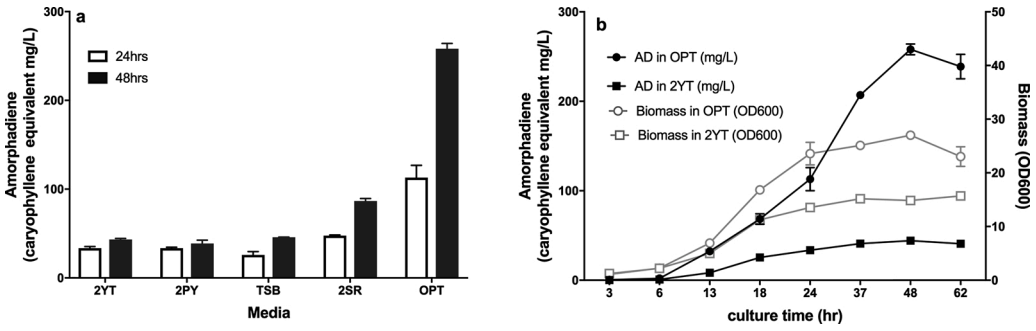

Fig. 7. Amorphadiene yield in commonly used medium and optimized medium (OPT). (**a**) Amorphadiene produced in different media. *B. subtilis* strain cGAF/SDFHCEGA was cultured in 1 mL of the four commonly used media and OPT, the yield of amorphadiene after 24 and 48 h was measured. (**b**) A curve of amorphadiene yield in 1 mL 2YT and OPT at different time points. Amorphadiene production (black lines) and optical density (grey lines) of *B. subtilis* cultured in 2YT and OPT in different time points was detected (n = 3).

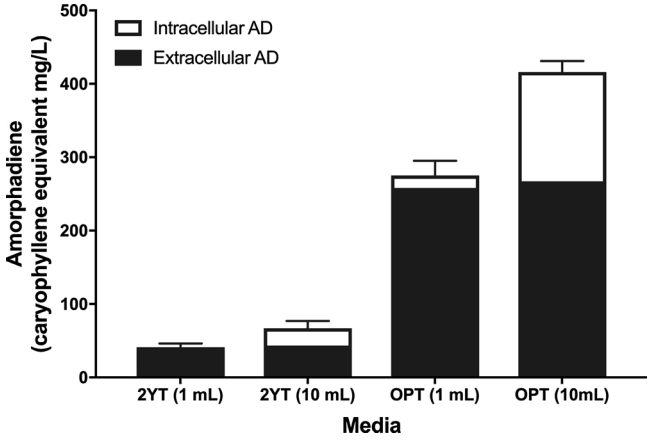

Fig. 8. Intracellular and extracellular amorphadiene produced in 1 or 10 mL cultures of cGAF/SDFHCEGA *B. subtilis* strain. Both intracellular and extracellular amorphadiene produced in 2YT and OPT cultures were measured. 1 mL cultures were grown in 14 mL Falcon round-bottom tube, while 100 mL Erlenmeyer flasks were used for 10 mL cultures. All amorphadiene samples were collected after 48 h of culture. Error bars indicate standard deviations of total amorphadiene (n = 3).

Discussion

Amorphadiene is the first committed sesquiterpene precursor in the biosynthesis of artemisinin (Fig. 1). With the high demand of artemisinin, the need for a sustainable method of production is a pressing issue. *E. coli* and *S. cerevisiae* have been engineered to produce high levels of artemisinin precursors, particularly artemisinic acid and amorphadiene, while similar metabolic engineering of *B. subtilis* for production of amorphadiene has lagged behind despite its high intrinsic capability to produce terpenoids. ADS has been co-expressed along with *dxs* and *idi*, two enzymes of the MEP pathway, in order to improve the production of amorphadiene in *B. subtilis* [6], but the final level achieved was only around 20 mg/L, much less than that by *E. coli* and *S. cerevisiae*. Hence, there is still room for improvement of amorphadiene production in *B. subtilis*. In this study, optimization steps encompassing enzyme modification, enhanced precursor supply and medium optimization have been explored, and resulted in an amorphadiene yield of 416 ± 15 mg/L, the highest reported in *B. subtilis* till now. This is 21-fold higher than the previously reported yield in *B. subtilis*, and more than twice the production in bench scale cultured *E. coli* and *S. cerevisiae* [48,49].

The first limiting factor for high amorphadiene production in *B. subtilis* is the poor expression of ADS [6]. A well-known method to optimize translation is adaptation of the *ads* sequence based on *B. subtilis* codon usage; however, this resulted in low expression of ADS [6]. An alternative approach is to optimize the folding and stability of the ADS protein. Here, *ads* expression was optimized by N-terminal fusion to GFP, which is known to be capable of increasing protein solubility and overall expression [50]. In addition, GFP fluorescent intensity could be used as a reporter for ADS expression. As seen in Fig. 3, the signal of GFP-ADS on the western blot was considerably improved compared to ADS alone, and amorphadiene production achieved was twice that previously reported in *B. subtilis* expressing ADS fused with an Arg_6 tag [6]. This improvement might be attributed to increased solubility, proper folding state or reduced degradation. It is possible that the *gfp* sequence is well adapted to the translation machinery of *B. subtilis*, and less likely to generate secondary structure of the mRNA, at the 5' end of the sequence, compared to *ads*. In addition, its proper folding can contribute to stabilization of ADS. Thus, the GFP fusion has a positive effect on the expression and stability of ADS in *B. subtilis*.

Further improvement of amorphadiene production was performed by enhancing the flux of the metabolic pathway and in turn increasing the supply of the C_5 building blocks of terpenoids. Overexpression of some enzymes of the MEP pathway for higher production of terpenoids has been previously conducted in both *E. coli* and *B. subtilis* [2,5,16,51]. In previous reports, the pHCMC04G plasmid demonstrated its ability to stably overexpress part of or all of the MEP pathway in *B. subtilis* leading to improved terpenoids yield [16,17]. To co-express the GFP-ADS fusion along with the pHCMC04G-containing MEP pathway genes in *B. subtilis*, an additional plasmid compatible with pHCMC04G was required and two vectors were tested here. One is the pBS0E theta replicating plasmid with different origin of replication and antibiotic resistance cassettes than pHCMC04G, while the other is pDR111 integrative plasmid for expression by integrating genes of interest into the genome of *B. subtilis*, providing higher stability than replicating plasmids [22,23,52,53]. As a result, when co-expressed with pHCMC04G constructs of the MEP pathway, the *B. subtilis* strains with *gfp-ads* genomically integrated manifested higher amounts of amorphadiene than those with replicative pBS0E (Fig. 4). Combination of a replicative plasmid with an integrative plasmid possessing a strong promoter is superior to the combination of two replicative plasmids [54]. Hence, the overexpression of four MEP pathway genes showed a certain degree of increase in amorphadiene where the cGA/CEGA strain produced 0.84 mg/L/OD and cGA/SDFH strain produced 1.36 mg/L/OD. The *B. subtilis* strain expressing all 7 MEP pathway genes and *ispA* along with chromosomally integrated *gfp-ads* caused a 4-fold increase in amorphadiene production (2.74 mg/L/OD) compared to cGA strain only expressing GFP-ADS fusion.

Moreover, higher levels of the sesquiterpene precursor FPP are required to further improve the production of amorphadiene. Expression of FPPS has been used to generate more substrate for ADS to improve amorphadiene production in *E. coli* or yeast, though not in *B. subtilis* [55,56]. As illustrated in Fig. 4, production of amorphadiene in strain cGAF/SDFHCEGA, which expressed FPPS and GFP-ADS fusion along with all the all the 7 MEP pathway enzymes and IspA, was increased to 3.41 mg/L/OD (42.51 mg/L), which is approximately 5-fold higher than the strains containing only GFP-ADS fusion. Note that, IspA enzyme carries out the function of FPPS to some extent but additional expression of *fpps* gene from *S. cerevisiae* further increased the supply of the

precursor FPP. Additionally, this strain showed sufficient segregational stability of the different constructs up to the 40th generation of cultivation to allow future large scale fermentation in the absence of antibiotics.

As the most promising *B. subtilis* strain for amorphadiene production was constructed successfully, further optimization of the culture conditions to boost the yield of amorphadiene was performed by the Design of Experiment (DoE) method [57], which can evaluate multiple variables systematically and simultaneously based on statistical analysis, and determine the optimal conditions with a minimal number of experiments. To date, it has been successfully used in optimization of fermentation variables for many practices in biotechnology such as enzyme production [58] and production of promising medical compounds in microorganisms [6,59]. Here, K_2HPO_4 and pyruvate were identified as the dominant factors influencing amorphadiene production. K_2HPO_4 may have a global metabolic effect on terpenoid production in *B. subtilis*, *E. coli* and yeast [6,48,51]. It served in the culture not only as a buffer but also as an ionic agent and source for phosphorus. When the MEP pathway genes were overexpressed in *B. subtilis*, lack of intracellular pyruvate substrate may have limited the efficiency of the pathway. To overcome this problem, pyruvate was added as a supplement to the medium leading to improved amorphadiene production as expected. Furthermore, it was reported that adding pyruvate and K_2HPO_4 to the growth medium of *B. subtilis* could drive the reactions in the MEP pathway towards terpenoid synthesis [51], which is in agreement with these results. Amorphadiene production by the optimum combination of these two factors was increased by 3-fold compared to that produced in non-optimized basic medium (from 83 mg/L to 258 mg/L).

Interestingly, when the cultures were scaled up from 1 mL (in 14 mL tubes) to 10 mL (in 100 mL flasks) using the optimized medium, similar extracellular amorphadiene (~260 mg/L) was observed, but intracellular amorphadiene was dramatically increased from 17 mg/L up to 150 mg/L. It is a common finding that many target compounds accumulate intracellularly, and as a result the yield can reach saturation which may limit further production [60,61]. In *E. coli*, amorphadiene production was improved by efflux transporter engineering [61,62], nevertheless, in *B. subtilis*, this is the first report of intracellular amorphadiene. Compared to *E. coli*, in *B. subtilis*, as a gram-positive organism, the secretion of specific target compounds might be hampered by the thickness of its cell wall [63]. Therefore, further improvement of amorphadiene production might be attained by enhancing its export from the cell.

Conclusion

The improvement of ADS expression by means of GFP fusion in *B. subtilis* is reported. The production level of amorphadiene was upregulated by overexpression of FPPS together with the complete MEP pathway, reaching 416 ± 15 mg/L in optimized medium, which is currently the highest yield of amorphadiene reported in *B. subtilis*. The engineered *B. subtilis* strain for amorphadiene production, as well as investigation of intracellular amorphadiene, can serve as a starting point for further scale-up of aerobic cultures, from shake flasks to batch fermentors [64]. Hence, using higher biomass concentrations and controlled fermentor conditions including a two-phase reactor design, *B. subtilis* can be utilized as an efficient cell factory for high-value terpenoid production.

Acknowledgments

Funding for this work was obtained through EuroCoRes SYNBIO (SYNMET), NWO-ALW 855.01.161 and EU FP-7 grant 289540 (PROMYSE). HP is recipient of Bernoulli scholarship.

We thank Pieter G. Tepper for the valuable discussions and advice on GC–MS measurements of amorphadiene.

Appendix A. Supplementary data

Supplementary material related to this article can be found, in the online version, at doi:https://doi.org/10.1016/j.nbt.2020.10.007.

References

[1] Abdallah II, Quax WJ. A glimpse into the biosynthesis of terpenoids. KnE Life Sci 2017;3:81. https://doi.org/10.18502/kls.v3i5.981.
[2] Ajikumar PK, Xiao W-H, Tyo KEJ, Wang Y, Simeon F, Leonard E, et al. Isoprenoid pathway optimization for Taxol precursor overproduction in *Escherichia coli*. Science 2010;330:70–4. https://doi.org/10.1126/science.1191652.
[3] Connolly JD, Hill RA. Dictionary of terpenoids. First. London: Chapman & Hall; 1991. https://doi.org/10.1007/978-1-4899-4513-6.
[4] Julsing MK, Koulman A, Woerdenbag HJ, Quax WJ, Kayser O. Combinatorial biosynthesis of medicinal plant secondary metabolites. Biomol Eng 2006;23:265–79. https://doi.org/10.1016/j.bioeng.2006.08.001.
[5] Martin VJJ, Pitera DJ, Withers ST, Newman JD, Keasling JD. Engineering a mevalonate pathway in *Escherichia coli* for production of terpenoids. Nat Biotechnol 2003;21:796–802. https://doi.org/10.1038/nbt833.
[6] Zhou K, Zou R, Zhang C, Stephanopoulos G, Too H-P. Optimization of amorphadiene synthesis in *Bacillus subtilis* via transcriptional, translational, and media modulation. Biotechnol Bioeng 2013;110:2556–61. https://doi.org/10.1002/bit.24900.
[7] Klein-Marcuschamer D, Ajikumar PK, Stephanopoulos G. Engineering microbial cell factories for biosynthesis of isoprenoid molecules: beyond lycopene. Trends Biotechnol 2007;25:417–24. https://doi.org/10.1016/j.tibtech.2007.07.006.
[8] Wagner WP, Helmig D, Fall R. Isoprene biosynthesis in *Bacillus subtilis* via the methylerythritol phosphate pathway. J Nat Prod 2000;63:37–40. https://doi.org/10.1021/np990286p.
[9] Withers ST, Keasling JD. Biosynthesis and engineering of isoprenoid small molecules. Appl Microbiol Biotechnol 2007;73:980–90. https://doi.org/10.1007/s00253-006-0593-1.
[10] Muntendam R, Melillo E, Ryden A, Kayser O. Perspectives and limits of engineering the isoprenoid metabolism in heterologous hosts. Appl Microbiol Biotechnol 2009;84:1003–19. https://doi.org/10.1007/s00253-009-2150-1.
[11] Koehn FE, Carter GT. The evolving role of natural products in drug discovery. Nat Rev Drug Discov 2005;4:206–20. https://doi.org/10.1038/nrd1657.
[12] Paddon CJ, Keasling JD. Semi-synthetic artemisinin: a model for the use of synthetic biology in pharmaceutical development. Nat Rev Microbiol 2014;12:355–67. https://doi.org/10.1038/nrmicro3240.
[13] World Health Organization. Global malaria diagnostic and artemisinin treatment commodities demand forecast 2017 – 2021. 2018. https://unitaid.org/assets/Global-malaria-diagnostic-and-artemisinin-treatment-commodities-demand-forecast-2017-–-2021-Report-May-2018.pdf.
[14] Paddon CJ, Westfall PJ, Pitera DJ, Benjamin K, Fisher K, McPhee D, et al. High-level semi-synthetic production of the potent antimalarial artemisinin. Nature 2013;496:528–32. https://doi.org/10.1038/nature12051.
[15] Guan Z, Xue D, Abdallah II, Dijkshoorn L, Setroikromo R, Lv G, et al. Metabolic engineering of *Bacillus subtilis* for terpenoid production. Appl Microbiol Biotechnol 2015;99:9395–406. https://doi.org/10.1007/s00253-015-6950-1.
[16] Xue D, Abdallah II, de Haan IEM, Sibbald MJJB, Quax WJ. Enhanced C_{30} carotenoid production in *Bacillus subtilis* by systematic overexpression of MEP pathway genes. Appl Microbiol Biotechnol 2015;99:5907–15. https://doi.org/10.1007/s00253-015-6531-3.
[17] Abdallah II, Pramastya H, van Merkerk R, Sukrasno, Quax WJ. Metabolic engineering of *Bacillus subtilis* toward taxadiene biosynthesis as the first committed step for taxol production. Front Microbiol 2019;10:218. https://doi.org/10.3389/fmicb.2019.00218.
[18] Dong H, Zhang D. Current development in genetic engineering strategies of Bacillus species. Microb Cell Fact 2014;13:63. https://doi.org/10.1186/1475-2859-13-63.
[19] Toymentseva AA, Altenbuchner J. New CRISPR-Cas9 vectors for genetic modifications of Bacillus species. FEMS Microbiol Lett 2019:366. https://doi.org/10.1093/femsle/fny284. fny284.
[20] Castillo-Hair SM, Fujita M, Igoshin OA, Tabor JJ. An Engineered *B. subtilis* inducible promoter system with over 10 000-Fold dynamic range. ACS Synth Biol 2019;8:1673–8. https://doi.org/10.1021/acssynbio.8b00469.
[21] Guiziou S, Sauveplane V, Chang H-J, Clerté C, Declerck N, Jules M, et al. A part toolbox to tune genetic expression in *Bacillus subtilis*. Nucleic Acids Res 2016;44:7495–508. https://doi.org/10.1093/nar/gkw624.
[22] Overkamp W, Beilharz K, Detert Oude Weme R, Solopova A, Karsens H, Kovács ÁT, et al. Benchmarking various green fluorescent protein variants in *Bacillus subtilis*, *Streptococcus pneumoniae*, and *Lactococcus lactis* for live cell imaging. Appl Environ Microbiol 2013;79:6481–90. https://doi.org/10.1128/AEM.02033-13.
[23] Popp PF, Dotzler M, Radeck J, Bartels J, Mascher T. The Bacillus BioBrick Box 2.0: expanding the genetic toolbox for the standardized work with *Bacillus subtilis*. Sci Rep 2017;7:15058. https://doi.org/10.1038/s41598-017-15107-z.
[24] Radeck J, Meyer D, Lautenschläger N, Mascher T. Bacillus SEVA siblings: a golden gate-based toolbox to create personalized integrative vectors for *Bacillus subtilis*. Sci Rep 2017;7:14134. https://doi.org/10.1038/s41598-017-14329-5.
[25] Radeck J, Kraft K, Bartels J, Cikovic T, Dürr F, Emenegger J, et al. The *Bacillus* BioBrick Box: generation and evaluation of essential genetic building blocks for

standardized work with *Bacillus subtilis*. J Biol Eng 2013;7:29. https://doi.org/10.1186/1754-1611-7-29.
[26] Martin VJJ, Yoshikuni Y, Keasling JD. The in vivo synthesis of plant sesquiterpenes by *Escherichia coli*. Biotechnol Bioeng 2001;75:497–503. https://doi.org/10.1002/bit.10037.
[27] Chang MCY, Eachus RA, Trieu W, Ro DK, Keasling JD. Engineering Escherichia coli for production of functionalized terpenoids using plant P450s. Nat Chem Biol 2007;3:274–7. https://doi.org/10.1038/nchembio875.
[28] Huang Q, Roessner CA, Croteau R, Scott AI. Engineering *Escherichia coli* for the synthesis of taxadiene, a key intermediate in the biosynthesis of taxol. Bioorg Med Chem 2001;9:2237–42. https://doi.org/10.1016/S0968-0896(01)00072-4.
[29] Biggs BW, Lim CG, Sagliani K, Shankar S, Stephanopoulos G, De Mey M, et al. Overcoming heterologous protein interdependency to optimize P450-mediated Taxol precursor synthesis in *Escherichia coli*. Proc Natl Acad Sci U S A 2016;113:3209–14. https://doi.org/10.1073/pnas.1515826113.
[30] Dyson MR, Shadbolt SP, Vincent KJ, Perera RL, McCafferty J. Production of soluble mammalian proteins in *Escherichia coli*: identification of protein features that correlate with successful expression. BMC Biotechnol 2004;4:1–18. https://doi.org/10.1186/1472-6750-4-32.
[31] Kim CW, Han KS, Ryu K-S, Kim BH, Kim K-HK-H, Choi Il S, et al. N-terminal domains of native multidomain proteins have the potential to assist de novo folding of their downstream domains in vivo by acting as solubility enhancers. Protein Sci 2007;16:635–43. https://doi.org/10.1110/ps.062330907.
[32] Panavas T, Sanders C, Butt TR. SUMO fusion technology for enhanced protein production in prokaryotic and eukaryotic expression systems. In: Ulrich HD, editor. Methods mol. Biol, vol. 497. Totowa, NJ: Humana Press; 2009. p. 303–17. https://doi.org/10.1007/978-1-59745-566-4_20.
[33] Quan J, Tian J. Circular polymerase extension cloning for high-throughput cloning of complex and combinatorial DNA libraries. Nat Protoc 2011;6:242–51. https://doi.org/10.1038/nprot.2010.181.
[34] Rodriguez S, Kirby J, Denby CM, Keasling JD. Production and quantification of sesquiterpenes in *Saccharomyces cerevisiae*, including extraction, detection and quantification of terpene products and key related metabolites. Nat Protoc 2014;9:1980–96. https://doi.org/10.1038/nprot.2014.132.
[35] Shao H, Cao Q, Zhao H, Tan X, Feng H. Construction of novel shuttle expression vectors for gene expression in *Bacillus subtilis* and *Bacillus pumilus*. J Gen Appl Microbiol 2015;61:124–31. https://doi.org/10.2323/jgam.61.124.
[36] Abdallah II, Xue D, Pramastya H, van Merkerk R, Setroikromo R, Quax WJ. A regulated synthetic operon facilitates stable overexpression of multigene terpenoid pathway in *Bacillus subtilis*. J Ind Microbiol Biotechnol 2020;47:243–9. https://doi.org/10.1007/s10295-019-02257-4.
[37] Wallaart TE, Bouwmeester HJ, Hille J, Poppinga L, Maijers NCAA. Amorpha-4,11-diene synthase: cloning and functional expression of a key enzyme in the biosynthetic pathway of the novel antimalarial drug artemisinin. Planta 2001;212:460–5. https://doi.org/10.1007/s004250000428.
[38] Anderson MS, Yarger JG, Burck CL, Poulter CD. Farnesyl diphosphate synthetase. Molecular cloning, sequence, and expression of an essential gene from Saccharomyces cerevisiae. J Biol Chem 1989;264. 19176–84. PMID: 2681213.
[39] Kunst F, Ogasawara N, Moszer I, Albertini AM, Alloni G, Azevedo V, et al. The complete genome sequence of the gram-positive bacterium *Bacillus subtilis*. Nature 1997;390:249–56. https://doi.org/10.1038/36786.
[40] Barbe V, Cruveiller S, Kunst F, Lenoble P, Meurice G, Sekowska A, et al. From a consortium sequence to a unified sequence: the *Bacillus subtilis* 168 reference genome a decade later. Microbiology 2009;155:1758–75. https://doi.org/10.1099/mic.0.027839-0.
[41] Borriss R, Danchin A, Harwood CR, Médigue C, Rocha EPC, Sekowska A, et al. *Bacillus subtilis*, the model Gram-positive bacterium: 20 years of annotation refinement. Microb Biotechnol 2018;11:3–17. https://doi.org/10.1111/1751-7915.13043.
[42] Belda E, Sekowska A, Le Fèvre F, Morgat A, Mornico D, Ouzounis C, et al. An updated metabolic view of the *Bacillus subtilis* 168 genome. Microbiology 2013;159:757–70. https://doi.org/10.1099/mic.0.064691-0.
[43] Bouwmeester HJH, Wallaart TETE, Janssen MHAa, van Loo B, Jansen BJMM, Posthumus MA, et al. Amorpha-4,11-diene synthase catalyses the first probable step in artemisinin biosynthesis. Phytochemistry 1999;52:843–54. https://doi.org/10.1016/S0031-9422(99)00206-X.
[44] Baadhe RR, Mekala NK, Parcha SR, Prameela Devi Y. Combination of ERG9 repression and enzyme fusion technology for improved production of amorphadiene in *Saccharomyces cerevisiae*. J Anal Methods Chem 2013;2013:1–8. https://doi.org/10.1155/2013/140469.
[45] Ma SM, Garcia DE, Redding-Johanson AM, Friedland GD, Chan R, Batth TS, et al. Optimization of a heterologous mevalonate pathway through the use of variant HMG-CoA reductases. Metab Eng 2011;13:588–97. https://doi.org/10.1016/j.ymben.2011.07.001.
[46] Vyas VV, Gupta S, Sharma P. Stability of a recombinant shuttle plasmid in *Bacillus subtilis* and *Escherichia coli*. Enzyme Microb Technol 1994;16:240–6. https://doi.org/10.1016/0141-0229(94)90049-3. PMID - 7764600.
[47] Zhao X, Xu J, Tan M, Zhen J, Shu W, Yang S, et al. High copy number and highly stable *Escherichia coli–Bacillus subtilis* shuttle plasmids based on pWB980. Microb Cell Fact 2020;19:25. https://doi.org/10.1186/s12934-020-1296-5.
[48] Baadhe RR, Mekala NK, Rao Parcha S, Prameela Devi Y. Optimization of amorphadiene production in engineered yeast by response surface methodology. 3 Biotech 2014;4:317–24. https://doi.org/10.1007/s13205-013-0156-y.
[49] Zhang C, Zou R, Chen X, Stephanopoulos G, Too H-P. Experimental design-aided systematic pathway optimization of glucose uptake and deoxyxylulose phosphate pathway for improved amorphadiene production. Appl Microbiol Biotechnol 2015;99:3825–37. https://doi.org/10.1007/s00253-015-6463-y.
[50] Waldo GS, Standish BM, Berendzen J, Terwilliger TC. Rapid protein-folding assay using green fluorescent protein. Nat Biotechnol 1999;17:691–5. https://doi.org/10.1038/10904.
[51] Zhang C, Chen X, Zou R, Zhou K, Stephanopoulos G, Too H-P. Combining genotype improvement and statistical media optimization for isoprenoid production in *E. coli*. PLoS One 2013;8:e75164. https://doi.org/10.1371/journal.pone.0075164.
[52] Ben-Yehuda S, Rudner DZ, Losick R. RacA, a bacterial protein that anchors chromosomes to the cell poles. Science 2003;299:532–6. https://doi.org/10.1126/science.1079914.
[53] Nguyen HD, Nguyen QA, Ferreira RC, Ferreira LCS, Tran LT, Schumann W. Construction of plasmid-based expression vectors for *Bacillus subtilis* exhibiting full structural stability. Plasmid 2005;54:241–8. https://doi.org/10.1016/j.plasmid.2005.05.001.
[54] Lynch M, Marinov GK. The bioenergetic costs of a gene. Proc Natl Acad Sci 2015:201514974. https://doi.org/10.1073/pnas.1514974112.
[55] Banyai W, Kirdmanee C, Mii M, Supaibulwatana K. Overexpression of farnesyl pyrophosphate synthase (FPS) gene affected artemisinin content and growth of *Artemisia annua* L. Plant Cell. Plant Cell Tiss Organ Cult 2010;103:255–65. https://doi.org/10.1007/s11240-010-9775-8.
[56] Dhar MK, Koul A, Kaul S. Farnesyl pyrophosphate synthase: a key enzyme in isoprenoid biosynthetic pathway and potential molecular target for drug development. N Biotechnol 2013;30:114–23. https://doi.org/10.1016/j.nbt.2012.07.001.
[57] Kumar V, Bhalla A, Rathore AS. Design of experiments applications in bioprocessing: concepts and approach. Biotechnol Prog 2014;30:86–99. https://doi.org/10.1002/btpr.1821.
[58] Hajji M, Rebai A, Gharsallah N, Nasri M. Optimization of alkaline protease production by *Aspergillus clavatus* ES1 in *Mirabilis jalapa* tuber powder using statistical experimental design. Appl Microbiol Biotechnol 2008;79:915–23. https://doi.org/10.1007/s00253-008-1508-0.
[59] Su W-T, Chen W-J, Lin Y-F. Optimizing emulsan production of *A. venetianus* RAG-1 using response surface methodology. Appl Microbiol Biotechnol 2009;84:271–9. https://doi.org/10.1007/s00253-009-1957-0.
[60] Dunlop MJ, Dossani ZY, Szmidt HL, Chu HC, Lee TS, Keasling JD, et al. Engineering microbial biofuel tolerance and export using efflux pumps. Mol Syst Biol 2011;7:487. https://doi.org/10.1038/msb.2011.21.
[61] Wang J-F, Xiong Z-Q, Li S-Y, Wang Y. Enhancing isoprenoid production through systematically assembling and modulating efflux pumps in *Escherichia coli*. Appl Microbiol Biotechnol 2013;97:8057–67. https://doi.org/10.1007/s00253-013-5062-z.
[62] Zhang C, Chen X, Stephanopoulos G, Too H-P. Efflux transporter engineering markedly improves amorphadiene production in Esch*erichia coli*. Biotechnol Bioeng 2016;113:1755–63. https://doi.org/10.1002/bit.25943.
[63] Thwaite JE, Baillie LWJ, Carter NM, Stephenson K, Rees M, Harwood CR, et al. Optimization of the cell wall microenvironment allows increased production of recombinant *Bacillus anthracis* protective antigen from *B. Subtilis*. Appl Environ Microbiol 2002;68:227–34. https://doi.org/10.1128/AEM.68.1.227-234.2002.
[64] Seletzky JM, Noak U, Fricke J, Welk E, Eberhard W, Knocke C, et al. Scale-up from shake flasks to fermenters in batch and continuous mode with *Corynebacterium glutamicum* on lactic acid based on oxygen transfer and pH. Biotechnol Bioeng 2007;98:800–11. https://doi.org/10.1002/bit.21359.